Hindawi
International Journal of Antennas and Propagation
Volume 2018, Article ID 4198243, 6 pages
https://doi.org/10.1155/2018/4198243

Research Article

A Full-Dielectric Chiral Material Based on a Honeycomb Structure

Ismael Barba,[1] **Ana Grande**,[1] **Gregorio J. Molina-Cuberos**,[2] **Ángel J. García-Collado**,[3] **José Represa**,[1] **and Ana C. L. Cabeceira**[1]

[1]*Departamento de Electricidad y Electrónica, Universidad de Valladolid, 47071 Valladolid, Spain*
[2]*Departamento de Física, Universidad de Murcia, 30071 Murcia, Spain*
[3]*Departamento de C. Politécnicas, Universidad Católica San Antonio, Murcia, Spain*

Correspondence should be addressed to Ismael Barba; ibarba@ee.uva.es

Received 28 March 2018; Revised 12 June 2018; Accepted 28 June 2018; Published 13 November 2018

Academic Editor: Giuseppe Castaldi

A uniaxial bianisotropic, full-dielectric structure has been designed and numerically studied. The material is based on a previously published 2D-honeycomb structure. A 3D expansion leads to an effective metamaterial showing a typical chiral electromagnetic behavior, i.e., a resonant electromagnetic activity with a small circular dichroism.

1. Introduction

Hexagonal structures with sixfold symmetry (also known as "honeycombs") have been widely used in different sectors, such as aerospace or construction, thanks to their special properties (mechanical, optical, thermal, etc.) [1, 2]. In 1989, Wojciechowski and Brańka proposed a "tilted" honeycomb, with sixfold symmetry but no mirror symmetry in a plane (that is, it is chiral in a plane, but not in the 3D space), as a way to obtain a negative Poisson's ratio [3]. That means that, contrary to regular honeycombs, it expands in all directions when it is pulled in only one of them. Structures of this kind are called "auxetic" honeycombs. Other implications of their geometrical chirality, in terms of mechanical properties, have been studied, like enhanced compressive strength capabilities, shear stiffness compared to classical centrosymmetric honeycomb configurations, or a synclastic curvature feature [1, 4].

From an electromagnetic point of view, chiral structures are known for their potential to show a reciprocal electromagnetic cross-coupling in their effective constitutive relations (bi-isotropy or bianisotropy) [5]. This property leads to different possible effects: first, the eigenmodes of a plane wave travelling through such materials are left- and right-handed circular polarized (LCP and RCP, respectively) waves [6]. Consequences of this effect are a rotation of the polarization angle when the travelling wave is linearly polarized (optical/electromagnetic activity), as well as a polarization change from lineal to elliptical and, eventually, circular [5]. Furthermore, in 2004, it was predicted that materials with strong electromagnetic activity can also possess a negative refractive index [7], and since then, several chiral metamaterial (CM) designs have been proposed and probed to produce such a negative refractive index [8, 9].

In 2009, David et al. proposed the application of a chiral honeycomb in electromagnetic absorbers [10]; later, in 2010, Kopyt et al. studied the electromagnetic behavior of such structure implemented with dielectrics (polymers), in order to check whether their structural chirality translates into chiral electromagnetic behavior (bianisotropy) [1], with negative results. That is, the structural chirality of the investigated honeycombs did not induce electromagnetic chirality effects.

Nevertheless, it is necessary to mention that they characterized a single layer of a two-dimensional structure (see Figure 1): though chirality may be defined in a plane geometry [11, 12], a planar structure cannot be chiral in the 3D space. Extensive research on the subject of such "planar chirality" has been done in recent years, demonstrating that electromagnetic bianisotropy requires a 3D geometrical chirality [13–18]. In some cases, "planar" chiral structures are actually three dimensional because of the presence of a

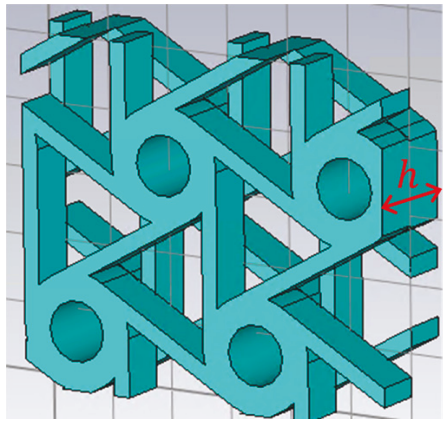

(a)

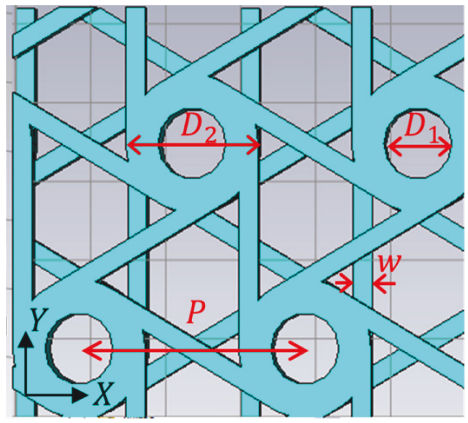

(b)

Figure 1: Geometry of the bilayered chiral structure under study. It is composed of two layers: the top layer is similar to the ones studied in [1, 9] and the second layer is the specular image of the first one. 3D view (a) and front view (b) of the structure.

dielectric substrate under the metal plane [13]. Other polarization phenomena have been observed in planar structures but being an essentially different phenomenon that leads to an asymmetric transmission. In that case, the perceived rotation of a "planar chiral" object is reversed if observed from opposite sides. This is in contrast with 3D chirality, where the sense of such rotation does not change upon reversal of the observation direction [16]; in this case, the eigenmodes are two corotating elliptical polarizations, instead of contrarotating circular polarizations, as in 3D chiral (bi-isotropic) materials [14, 19]. This "asymmetric transmission" is a dissipative effect and can only be observed in lossy anisotropic structures [16], while the structures studied in [1, 10] are isotropic in the plane.

It is worth of noticing that, among other alternatives, three-dimensional chirality may be achieved by means of planar structures, if several layers of the structure are used, through electromagnetic coupling between the different layers [20–26]. A bilayered, metallic, chiral honeycomb was studied in [27], and electromagnetic activity was found. In this work, we have performed an electromagnetic analysis of a full-dielectric chiral honeycomb made by two layers, the second one being the specular image of the first one (see Figure 1). An all-dielectric implementation of a chiral structure may be particularly attractive due to their low losses, in comparison with implementations based on metal-dielectric interfaces [28].

The numerical analysis has been implemented by means of a CST Studio Suite® simulation. The first reflection coefficient minimum follows the classical half-wave transformer characteristics of homogenized panels. At higher frequencies, and before longitudinal components are induced, different chiral resonances appear. The effective Pasteur (chirality) parameter has been extracted from the S-parameters, showing a resonant behavior similar to the one found in other chiral structures (i.e., the Condon model) [5], but with low energy losses.

2. Chiral Bi-isotropic Media

In contrast to conventional isotropic materials, a chiral bi-isotropic medium (also known as "Pasteur" medium) is characterized by a cross-coupling between electric and magnetic fields, leading to constitutive relationships governed by the following equations:

$$\begin{aligned} \overrightarrow{D} &= \varepsilon \overrightarrow{E} - \frac{j\kappa}{c_0} \overrightarrow{H}, \\ \overrightarrow{B} &= \frac{j\kappa}{c_0} \overrightarrow{E} + \mu \overrightarrow{H}, \end{aligned} \tag{1}$$

where c_0 is the light speed in vacuum and κ is the "chirality" or "Pasteur" parameter and, as well as ε and μ, is a function of the frequency [5].

If we assume a plane wave travelling on such medium with a function $e^{j(kz-\omega t)}$, we can derive the eigenvalue equation, which has two solutions for the wavenumber k:

$$k_{\pm} = \frac{\omega}{c_0} (\sqrt{\varepsilon\mu} \pm \kappa), \tag{2}$$

where $k_{\pm}$ are the wavenumbers of RCP and LCP eigenwaves. A real part of the Pasteur parameter κ involves, then, a phase difference between both waves. Since a linearly polarized wave may be decomposed in two right- and left-handed polarized waves, it will suffer a rotation of its polarization angle ("electromagnetic activity") [29–31]:

$$\theta = k_0 z \kappa', \tag{3}$$

where z is the distance travelled by the plane wave and κ' the real part of the parameter κ. An imaginary part of κ involves a difference in absorption between both waves, so a linearly polarized plane wave will become elliptical and, eventually, circular ("circular dichroism"). If we define the ellipticity as the angle 2η whose tangent is the minor to major amplitude ratio of the polarization ellipse, then a plane wave, linearly

polarized in origin, will present after propagating a distance z an ellipticity given by [29–31]

$$\tan(2\eta) = \tanh\left(2k_0 z\kappa''\right). \quad (4)$$

3. Structure under Study

A chiral structure consisting of a network of hexachiral honeycombs, made by a distribution of equally spaced cylinders connected by segments of the same material (see Figure 1), has been studied. This structure is based on [1], but in this case, there are two layers of the network, the second one being the specular image of the first one with respect to a perpendicular plane. In both structures, the inner and outer diameters of the cylinders are $D_1 = 9$ mm and $D_2 = 17.5$ mm, respectively; the width of the segments connecting the cylinders is $w = 2.5$ mm; the distance between two cylinders (i.e., the period in the x-direction) is $P = 30$ mm; and the width of the whole structure is $h = 15$ mm.

The numerical analysis has been performed, as mentioned, by using CST Studio Suite®. The extracted S-parameters have been processed in order to retrieve the polarization angle and ellipticity of the transmitted wave [29–31]. Then, the effective parameters of the equivalent medium have been obtained using (3) and (4).

4. Results and Discussion

4.1. Broadband Simulation. In order to compare results, a first simulation was performed using a single honeycomb layer (that is, a structure similar to the ones studied in [1, 9]) with $h = 15$ mm. Periodical (unit cell) boundary conditions were used in the lateral walls. The electrical characteristics of the medium were $\varepsilon_r = 2.57$ $\tan\delta = 0.0039$, and $\mu_r = 1$ (these are the measured characteristics of a 3D-printed ABS medium [32]). The scattering parameters for perpendicular incidence are shown in Figure 2. Up to 12 Floquet modes were taken into account, in order to look for any higher space harmonics. Nevertheless, only the first two harmonics (that is, plane waves linearly polarized in the x- and y-directions) were found in the frequency band under study (0–16 GHz). Note that the minimum wavelength in this band would be around 12 mm. At the same time, the results do not depend on the direction of the polarization plane of the incident wave.

S_{11Co} and S_{21Co} are the scattering parameters in copolarization (i.e., they determine the components of the scattered wave parallel to the incident one), while $S_{11Cross}$ and $S_{21Cross}$ represent the scattering parameters in cross-polarization (components of the scattered wave perpendicular to the incident one). In the low-frequency limit (0–8 GHz), when the wavelength is much larger than the dimensions of the structures, the panel behaves as a homogeneous dielectric layer with an effective relative permittivity of 1.6, approximately. For frequencies higher than 8 GHz, several resonances appear. Still, cross-polarized parameters are always null, which means no electromagnetic activity or dichroism is found, and the medium behaves as nonchiral;

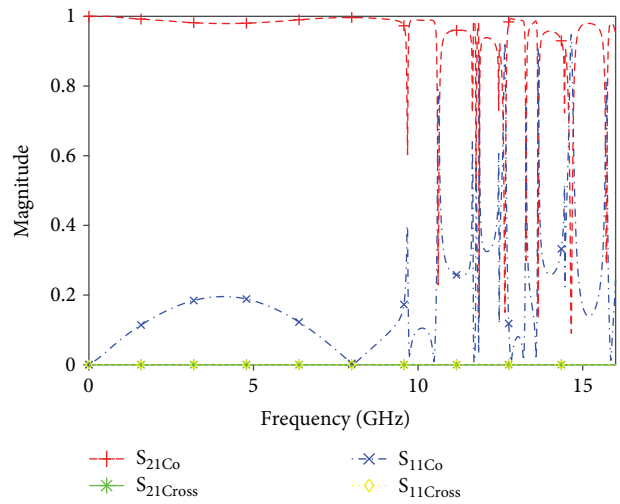

Figure 2: Scattering parameters (magnitude) for a linearly polarized plane wave, normally incident on a single layer chiral honeycomb.

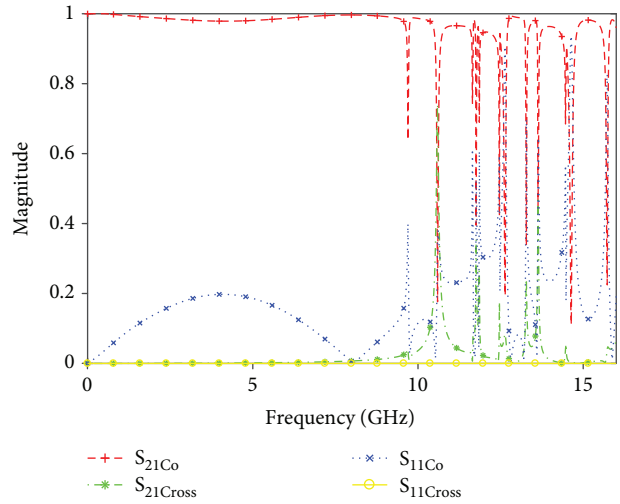

Figure 3: Scattering parameters (magnitude) for a linearly polarized plane wave, normally incident on a structure as shown in Figure 1.

as mentioned in the introduction, this result is consistent with previous results [1] and the predictions found in the literature [5, 6, 13, 16]. Similar results are obtained if a single honeycomb layer is placed on a uniform dielectric layer.

In the next simulation, a second layer was introduced (the model being as shown in Figure 1). Again, the scattering parameters for normal incidence and linear polarization have been computed, the results being depicted in Figure 3. It is worth mentioning that the scattering parameters are reciprocal and do not depend on the polarization angle of the incident wave.

In the lower frequencies (0–10 GHz), the results are virtually identical to the first case (Figure 2), but for frequencies higher than 10 GHz, some of the resonances involve cross-polarized transmission. This result (along with the lack of cross-polarized reflection) is a signal of electromagnetic activity and a uniaxial chiral behavior. A detailed view of

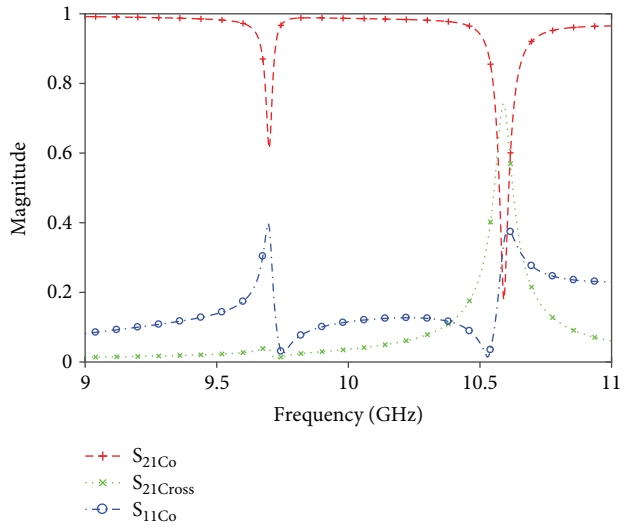

Figure 4: Scattering parameters (magnitude) for a linearly polarized plane wave, normally incident on a structure as shown in Figure 1. Zoom on the 9–11 GHz band.

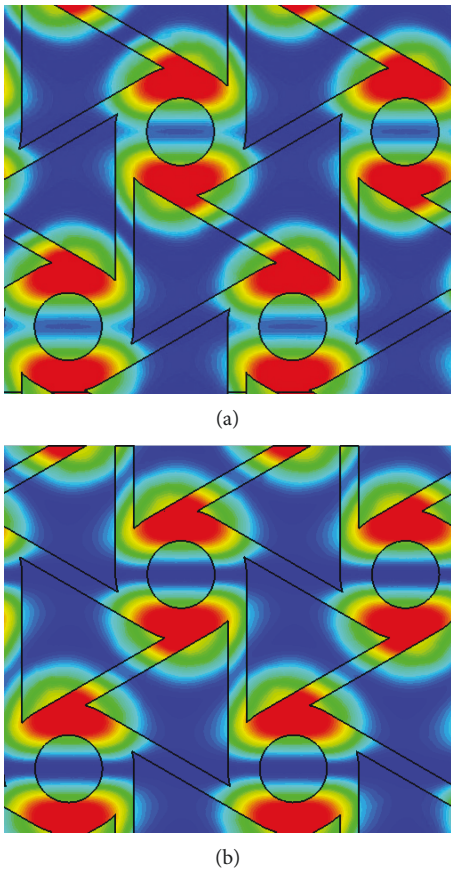

(a)

(b)

Figure 5: Electric energy density for a vertical polarized plane wave, at a frequency of 9.7 GHz: (a) first layer; (b) second layer.

the area between 9 and 11 GHz, including the first two resonant frequencies, is shown in Figure 4, where two resonances in the band 9–11 GHz can be observed. Both resonances are

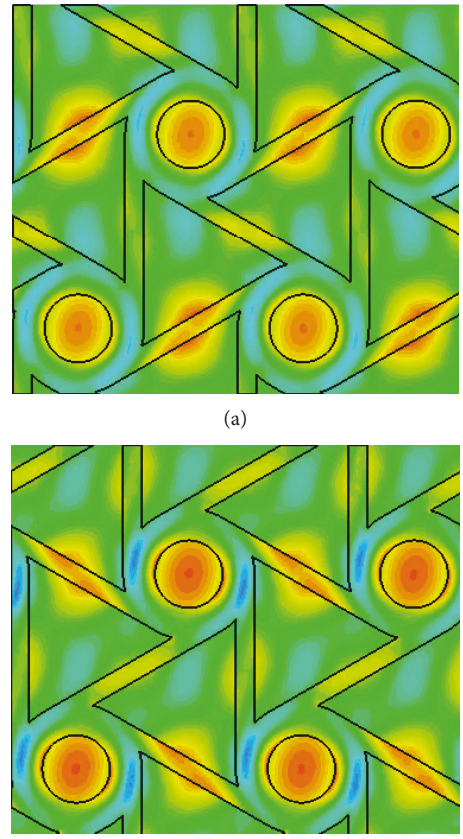

(a)

(b)

Figure 6: Electric energy density for a vertical polarized plane wave, at a frequency of 10.59 GHz: (a) first layer; (b) second layer.

also present in the nonchiral structure (Figure 2), but the second one, now, is associated, as mentioned, to a cross-polarized transmission. In order to find the physical mechanism that governs the chiral behavior of the structure, the electric field distribution in both resonant frequencies is shown in Figures 5 and 6.

Clearly, the first resonance (Figure 5) takes place in the cylinders (which are larger than the segments connecting them), the electric field being concentrated inside them. It is logical, then, that there is no significant difference between the chiral and the nonchiral structures, since the difference between them is in the arrangement of the segments connecting the cylinders. In the second resonant frequency, though, there is a concentration of electrical field inside these segments (Figure 6). We may deduce, then, that the electric coupling between those segments with different orientation is responsible for the cross-polarized coefficient and for the chiral behavior. In the nonchiral structure, they are parallel to each other, so the structure is equivalent to a single layer. By the same way, this coupling does not exist anymore if a single honeycomb layer is placed on a uniform dielectric layer, which explains why there is no electromagnetic activity in that case either.

In order to check whether this cross-polarized transmission corresponds to a rotation of the polarization plane (electromagnetic activity) or a change to elliptical polarization

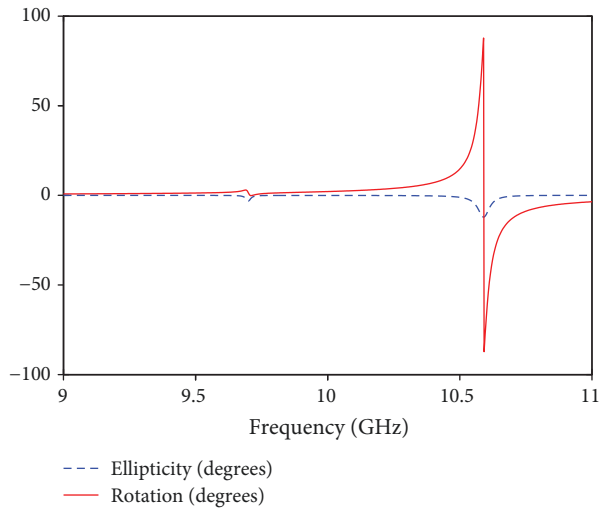

Figure 7: Rotation of the polarization plane and ellipticity of the transmitted wave after the data shown in Figure 4.

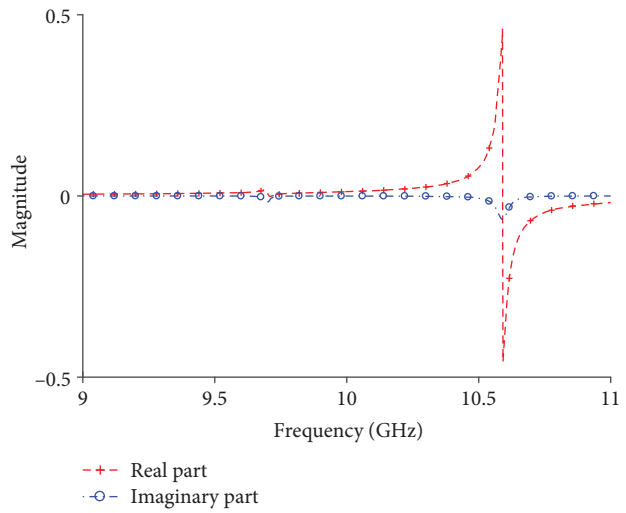

Figure 8: Frequency dependence of the effective Pasteur parameter, obtained from the data shown in Figure 7. Real and imaginary parts.

(circular dichroism), the rotation angle and ellipticity of the transmitted wave were computed, the results being shown in Figure 7.

The results show how, at the second resonance frequency, there is a high rotation of the polarization. Additionally, it appears to be an ellipticity that is relatively low compared with the rotation. That means there are low losses associated with the chirality and then low circular dichroism. The value of the equivalent Pasteur parameter can be calculated from this data, following (3) and (4). The results are shown in Figure 8, where we can see how the Pasteur parameter shows a second-order resonant behavior, with a resonance frequency at 10.58 GHz. The imaginary part of κ (responsible of the chiral losses and the circular dichroism, as seen in (4)) is much lower than the real part (responsible of the electromagnetic activity).

5. Conclusions

A full-dielectric chiral structure has been modelled and numerically studied. The structure is based on a preexistent chiral honeycomb. The results show no chiral effects for a single layer of the structure (which is consistent with previous results found in the literature); however, when two layers of opposite handedness are used, chirality symmetry appears and electromagnetic activity can be observed at microwave frequencies. Circular dichroism remains small, which means there are small losses associated with its chiral behavior.

Data Availability

The data that support the findings of this study are provided in the Results and Discussion of the article.

Conflicts of Interest

The authors declare that they have no conflicts of interest.

Acknowledgments

This work has been supported in part by the Spanish Government MINECO and the European Commission (ERDF) [Research Projects: TEC2014-55463-C3-1-P and TEC2014-55463-C3-2-P].

References

[1] P. Kopyt, R. Damian, M. Celuch, and R. Ciobanu, "Dielectric properties of chiral honeycombs – modelling and experiment," *Composites Science and Technology*, vol. 70, no. 7, pp. 1080–1088, 2010.

[2] S. Lee, S. Kim, T.-T. Kim et al., "Reversibly stretchable and tunable terahertz metamaterials with wrinkled layouts," *Advanced Materials*, vol. 24, no. 26, pp. 3491–3497, 2012.

[3] K. W. Wojciechowski and A. C. Brańka, "Negative Poisson ratio in a two-dimensional "isotropic" solid," *Physical Review A*, vol. 40, no. 12, pp. 7222–7225, 1989.

[4] D. Bornengo, F. Scarpa, and C. Remillat, "Evaluation of hexagonal chiral structure for morphing airfoil concept," *Proceedings of the Institution of Mechanical Engineers, Part G: Journal of Aerospace Engineering*, vol. 219, no. 3, pp. 185–192, 2005.

[5] I. V. Lindell, A. H. Sihvola, S. A. Tretyakov, and A. J. Viitanen, *Electromagnetic Waves on Chiral and Bi-Isotropic Media*, Artech House, Norwood, MA, USA, 1994.

[6] J. A. Kong, *Electromagnetic Wave Theory*, EMW Publishing, Cambridge, USA, 2008.

[7] J. B. Pendry, "A chiral route to negative refraction," *Science*, vol. 306, no. 5700, pp. 1353–1355, 2004.

[8] F. Fang and Y. Cheng, "Dual-band terahertz chiral metamaterial with giant optical activity and negative refractive index based on cross-wire structure," *Progress In Electromagnetics Research M*, vol. 31, pp. 59–69, 2013.

[9] G. J. Molina-Cuberos, Á. J. García-Collado, I. Barba, and J. Margineda, "Chiral metamaterials with negative refractive index composed by an eight-cranks molecule," *IEEE Antennas and Wireless Propagation Letters*, vol. 10, pp. 1488–1490, 2011.

[10] V. David, I. Nica, and A. Salceanu, "Electromagnetic absorbers based on chiral honeycomb slab," in *2009 International Symposium on Electromagnetic Compatibility - EMC Europe*, pp. 1–4, Athens, Greece, 2009.

[11] P. Le Guennec, "Two-dimensional theory of chirality. I. Absolute chirality," *Journal of Mathematical Physics*, vol. 41, no. 9, pp. 5954–5985, 2000.

[12] P. Le Guennec, "Two-dimensional theory of chirality. II. Relative chirality and the chirality of complex fields," *Journal of Mathematical Physics*, vol. 41, no. 9, pp. 5986–6006, 2000.

[13] M. Kuwata-Gonokami, N. Saito, Y. Ino et al., "Giant optical activity in quasi-two-dimensional planar nanostructures," *Physical Review Letters*, vol. 95, no. 22, 2005.

[14] V. A. Fedotov, P. L. Mladyonov, S. L. Prosvirnin, A. V. Rogacheva, Y. Chen, and N. I. Zheludev, "Asymmetric propagation of electromagnetic waves through a planar chiral structure," *Physical Review Letters*, vol. 97, no. 16, 2006.

[15] A. S. Schwanecke, V. A. Fedotov, V. V. Khardikov, S. L. Prosvirnin, Y. Chen, and N. I. Zheludev, "Nanostructured metal film with asymmetric optical transmission," *Nano Letters*, vol. 8, no. 9, pp. 2940–2943, 2008.

[16] E. Plum, V. A. Fedotov, and N. I. Zheludev, "Extrinsic electromagnetic chirality in metamaterials," *Journal of Optics A: Pure and Applied Optics*, vol. 11, no. 7, 2009.

[17] M. Esposito, V. Tasco, M. Cuscunà et al., "Nanoscale 3D chiral plasmonic helices with circular dichroism at visible frequencies," *ACS Photonics*, vol. 2, no. 1, pp. 105–114, 2015.

[18] X. Ma, M. Pu, X. Li, Y. Guo, P. Gao, and X. Luo, "Meta-chirality: fundamentals, construction and applications," *Nanomaterials*, vol. 7, no. 5, p. 116, 2017.

[19] Z. Li, M. Gokkavas, and E. Ozbay, "Manipulation of asymmetric transmission in planar chiral nanostructures by anisotropic loss," *Advanced Optical Materials*, vol. 1, no. 7, pp. 482–488, 2013.

[20] A. V. Rogacheva, V. A. Fedotov, A. S. Schwanecke, and N. I. Zheludev, "Giant gyrotropy due to electromagnetic-field coupling in a bilayered chiral structure," *Physical Review Letters*, vol. 97, no. 17, 2006.

[21] E. Plum, V. A. Fedotov, A. S. Schwanecke, N. I. Zheludev, and Y. Chen, "Giant optical gyrotropy due to electromagnetic coupling," *Applied Physics Letters*, vol. 90, no. 22, article 223113, 2007.

[22] J. Zhou, J. Dong, B. Wang, T. Koschny, M. Kafesaki, and C. M. Soukoulis, "Negative refractive index due to chirality," *Physical Review B*, vol. 79, no. 12, 2009.

[23] M. Decker, R. Zhao, C. M. Soukoulis, S. Linden, and M. Wegener, "Twisted split-ring-resonator photonic metamaterial with huge optical activity," *Optics Letters*, vol. 35, no. 10, pp. 1593–1595, 2010.

[24] M. Giloan, R. Gutt, and G. Saplacan, "Optical chiral metamaterial based on meta-atoms with three-fold rotational symmetry arranged in hexagonal lattice," *Journal of Optics*, vol. 17, no. 8, p. 085102, 2015.

[25] I. Barba, A. Grande, A. C. L. Cabeceira et al., "A complementary chiral metamaterial with giant electromagnetic activity and low losses," in *META Proceedings: 7th International Conference on Metamaterials, Photonic Crystals and Plasmonics (META'16)*, pp. 1585–1588, Torremolinos, Málaga, 2016.

[26] O. Fernández, A. Gómez, J. Basterrechea, and A. Vegas, "Reciprocal circular polarization handedness conversion using chiral metamaterials," *IEEE Antennas and Wireless Propagation Letters*, vol. 16, pp. 2307–2310, 2017.

[27] I. Barba, A. Grande, A. C. López-Cabeceira, and J. Represa, "A bi-isotropic hexachiral grid in PCB," in *2017 IEEE MTT-S International Conference on Numerical Electromagnetic and Multiphysics Modeling and Optimization for RF, Microwave, and Terahertz Applications (NEMO)*, pp. 254–256, Seville, Spain, 2017.

[28] A. Yahyaoui and H. Rmili, "Chiral all-dielectric metasurface based on elliptic resonators with circular dichroism behavior," *International Journal of Antennas and Propagation*, vol. 2018, Article ID 6352418, 7 pages, 2018.

[29] S. S. Oh and O. Hess, "Chiral metamaterials: enhancement and control of optical activity and circular dichroism," *Nano Convergence*, vol. 2, no. 1, p. 24, 2015.

[30] J. Lekner, "Optical properties of isotropic chiral media," *Pure and Applied Optics: Journal of the European Optical Society Part A*, vol. 5, no. 4, pp. 417–443, 1996.

[31] H.-B. Wang, X. Zhou, D.-F. Tang, and J.-F. Dong, "Diode-like broadband asymmetric transmission of linearly polarized waves based on Fabry–Perot-like resonators," *Journal of Modern Optics*, vol. 64, no. 7, pp. 750–759, 2017.

[32] C. Dichtl, P. Sippel, and S. Krohns, "Dielectric properties of 3D printed polylactic acid," *Advances in Materials Science and Engineering*, vol. 2017, Article ID 6913835, 10 pages, 2017.